http://dx.doi.org/10.5665/sleep.1706

Developmental Changes in Glutamatergic Fast Synaptic Neurotransmission in the Dorsal Subcoeruleus Nucleus

Christen Simon, BS; Abdallah Hayar, PhD; Edgar Garcia-Rill, PhD

Center for Translational Neuroscience, Department of Neurobiology and Developmental Sciences, University of Arkansas for Medical Sciences, Little Rock, AR

Study Objectives: The dorsal subcoeruleus nucleus (SubCD) is involved in the generation of rapid eye movement sleep (REM), a state distinguished by high-frequency EEG activity, muscle atonia, and ponto-geniculo-occipital (PGO) waves. Activation of the SubCD by injection of the glutamate (GLU) receptor agonist kainic acid (KA) produced a REM sleep-like state with muscle atonia. We tested the hypothesis that developmental changes in the GLU excitability of SubCD neurons could underlie the developmental decrease in REM sleep that occurs in the rat from postnatal days 10-30.

Design: Sagittal sections containing the SubCD were cut using 9-15 day old rat pups. Whole-cell patch clamp recordings were performed on SubCD neurons and responses were measured following electrical stimulation or bath application of the GLU receptor agonists N-methyl-D-aspartic acid (NMDA) or KA.

Measurements and Results: Pharmacological or electrical stimulation increased non-cholinergic excitatory postsynaptic currents (EPSCs) in SubCD neurons, which were blocked by GLU receptor antagonists. Although no developmental changes were observed in the relative contribution of AMPA/KA and NMDA receptors to the responses, there was a developmental decrease in the half-width duration of both evoked and miniature EPSCs. Bath application of NMDA or KA revealed a developmental decrease in the direct response of SubCD neurons to these agonists.

Conclusions: The SubCD receives glutamatergic input, which may be involved in activation of SubCD neurons during REM sleep. A developmental decrease in the glutamatergic excitability of these neurons could underlie the developmental decrease in REM sleep observed in humans and rodents.

Keywords: Arousal, development, dorsal subcoeruleus nucleus, glutamate, kainic acid, NMDA, rapid eye movement sleep

Citation: Simon C; Hayar A; Garcia-Rill E. Developmental changes in glutamatergic fast synaptic neurotransmission in the dorsal subcoeruleus nucleus. *SLEEP* 2012;35(3):407-417.

INTRODUCTION

Rapid eye movement (REM) sleep is distinguished by high-frequency, low-amplitude activity in the cortical EEG, muscle atonia, and ponto-geniculo-occipital (PGO) waves (P waves in the rat), which are field potentials that originate in the pons and travel to the lateral geniculate nucleus of the thalamus and visual cortex. Early studies discovered that injection of the non-specific acetylcholine (ACh) receptor agonist carbachol (CAR) into the brainstem of cats produced REM sleep with muscle atonia and PGO waves.[1,2] These studies were later reproduced in the rat, following injections into the dorsal subcoeruleus (SubCD) nucleus.[3] Activation of the SubCD by injections of the glutamate (GLU) receptor agonist kainic acid (KA), or the $GABA_A$ receptor antagonists gabazine (GBZ) and bicuculline (BIC) produced a REM sleep-like state with muscle atonia and PGO waves.[3-5] On the other hand, inactivation of the region by injections of the voltage-dependent sodium channel blocker tetrodotoxin (TTX) decreased REM sleep.[6]

The pedunculopontine nucleus (PPN), which contains separate populations of cholinergic, glutamatergic, and GABAergic neurons,[7] is one possible source of glutamatergic afferents to the SubCD.[8,9] The SubCD contains glutamatergic, and perhaps GABAergic, neurons.[10] Efferents of the SubCD project to a number of areas, including the medulla (involved in generating muscle atonia), the thalamus (involved in the generation of cortical oscillations and PGO waves), and the hippocampus (involved in learning and memory).[3]

Considering the importance of the SubCD in generating REM sleep,[3,4,6,11,12] perhaps developmental changes in excitation of the SubCD could underlie the developmental decrease in REM sleep in that occurs humans from birth until the end of puberty and in the rat from postnatal days 10 to 30.[13,14] Cholinergic neurotransmission has been thoroughly tested in the SubCD in vitro.[15,16] However, while glutamatergic neurotransmission has been found to be important for the generation of REM sleep,[4,10] the role of glutamatergic neurotransmission in the SubCD has yet to be tested in vitro. We tested the hypothesis that glutamatergic neurotransmission is important in the excitation of SubCD neurons, and developmental changes in glutamatergic neurotransmission in this nucleus may underlie the developmental decrease in REM sleep in the rat.

METHODS

All experimental protocols were approved by the Institutional Animal Care and Use Committee of the University of Arkansas for Medical Sciences and were in agreement with the National Institutes of Health guidelines for the care and use of laboratory animals.

Slice Preparation

Pups aged 9-15 days from adult timed-pregnant Sprague-Dawley rats (280-350 g) were anesthetized with ketamine (70

Submitted for publication June, 2011
Submitted in final revised form September, 2011
Accepted for publication September, 2011
Address correspondence to: E. Garcia-Rill, PhD, Director, Center for Translational Neuroscience, Department of Neurobiology and Developmental Sciences, University of Arkansas for Medical Sciences, Slot 847, 4301 West Markham Street, Little Rock, Arkansas 72205; Tel: (501) 686-5167; Fax: (501) 526-7928; E-mail: GarciaRillEdgar@uams.edu

mg/kg, IP) until tail pinch reflex was absent. This age was selected due to the developmental decrease in REM sleep that occurs in the rat during this period, which undergoes the most prominent changes by 15 days.[13] Pups were decapitated, and the brains were rapidly removed and cooled in oxygenated sucrose-artificial cerebrospinal fluid (sucrose-aCSF). The sucrose-aCSF consisted of (in mM): 233.7 sucrose, 26 $NaHCO_3$, 3 KCl, 8 $MgCl_2$, 0.5 $CaCl_2$, 20 glucose, 0.4 ascorbic acid, and 2 sodium pyruvate. 400 μm sagittal sections containing the SubCD were cut using a Vibratome 1000 plus with a 900R refrigeration system (Vibratome Instruments, St. Louis, MO). Slices were allowed to equilibrate in aCSF at room temperature for 1 h. Mg^{2+}-free aCSF was used for all of the experiments and was composed of (in mM): 117 NaCl, 4.7 KCl, 2.5 $CaCl_2$, 1.2 NaH_2PO_4, and 24.9 $NaHCO_3$, and 20 glucose.

Whole-Cell Patch Clamp Recordings

Whole-cell recordings were performed using borosilicate glass capillaries pulled on a Sutter P-97 puller (Sutter Instrument Company, Novato, CA) and filled with a solution of (in mM): 124 K-gluconate, 10 HEPES, 10 phosphocreatine di tris, 0.2 EGTA, 4 Mg_2ATP, 0.3 Na_2GTP, and 0.02% Lucifer yellow. Osmolarity was adjusted to 270-290 mOsm and pH to 7.4. The pipette resistance was 2-5 MΩ. Slices were recorded at 30°C while perfused (1.5 mL/min) with oxygenated (95% O_2- 5% CO_2) aCSF in an immersion chamber. No series resistance compensation was performed in this study. Neurons were visualized using an upright microscope (Nikon FN-1 with X40 water immersion lens, X1-2 magnifying turret, and Gibraltar platform; Nikon Instruments, Melville, NY) equipped for epifluorescence and near-infrared differential interference contrast optics. The anatomical location of recorded cells within the SubCD was confirmed using a 4X objective lens before and after recording. Analog signals were low-pass filtered at 2 kHz using a Multiclamp 700B amplifier and digitized at 5 kHz using a Digidata-1440A converter and pClamp10 software (Molecular Devices, Union City, CA). Drugs were administered to the slice by bath application via a peristaltic pump (Cole-Parmer, Vernon Hills, IL) and a 3-way valve system.

To determine the intrinsic membrane properties of cells, depolarizing and hyperpolarizing current (resting membrane potential = −60 mV; −180 to 90 pA, 30 pA steps, 500 ms duration) or voltage steps (holding potential, HP = −60 mV; −120 to −10 mV, 15 mV steps, 500 ms duration) were applied under current-clamp and voltage-clamp configurations. To test the effects of neuroactive agents, cells were held at −60 mV in voltage clamp mode, and every 20 sec, the membrane potential was held at a hyperpolarized level (HP = −120 mV) for 200 ms to determine changes in input resistance (R_{in}). The membrane capacitance was determined using the equation $C = \tau / R$, where τ represents the membrane time constant (determined by fitting an exponential decay curve to the initial portion of the voltage response to injection of a −40 pA current step), and R represents the membrane input resistance (determined by measuring the voltage change in response to a −40 pA current step according to Ohm's law [$R = V / I$]).

For recording spontaneous, electrically evoked, and miniature excitatory postsynaptic currents (EPSCs), the membrane potential was held at −70 mV to prevent the generation of action potentials. Furthermore, for recording electrically evoked EPSCs, a hyperpolarizing step from −70 to −120 was applied every 10 sec to determine changes in R_{in}.

Electrical Stimulation

To evoke EPSCs, electrical stimulation was applied using a bipolar tungsten microelectrode (200 kΩ resistance, 50 μm diameter) driven by a constant current stimulus isolation unit (Digitimer Ltd., Hertfordshire, England). Pulse duration was 0.1 msec and stimulation voltage was adjusted to evoke a consistent response with no failure rate (1.5-1.7 times threshold). For local stimulation studies, the stimulation electrode was placed in the SubCD 50-200 μm away from the recorded neuron.

Drug Application

Bath-applied solutions reached the slice 1.5 min after the start of application. Drugs used in this study included the GLU receptor agonists kainic acid (KA, 1 μM) and N-methyl-D-aspartic acid (NMDA, 4 μM), the sodium channel blocker tetrodotoxin citrate (TTX, 1 μM), the selective NMDA receptor antagonist 2-amino-5-phosphonovaleric acid (APV, 50 μM), the KA and 2-amino-3-(5-methyl-3-oxo-1,2-oxazol-4-yl) propanoic acid (AMPA) receptor antagonist 6-cyano-7-nitroquinoxaline-2, 3-dione (CNQX, 10 μM), the $GABA_A$ receptor antagonist gabazine (GBZ, 10 μM), the glycine receptor antagonist strychnine (STR, 10 μM), the nicotinic ACh receptor antagonist mecamylamine (MEC, 10 μM), and the muscarinic ACh receptor antagonist atropine (ATR, 10 μM). All drugs were purchased from Sigma (St. Louis, MO) except TTX, which was purchased from Tocris Bioscience (Ellisville, MO).

Data Analysis

Off-line analyses were performed using Clampfit 10 software (Molecular Devices, Sunnyvale, CA). Only cells with action potential amplitudes higher than 45 mV and resting membrane potentials more negative than −45 mV were included in the analyses. Developmental changes were determined using Student's *t*-tests with OriginPro 8.0 software (OriginLab Corporation, Northampton, MA). For spontaneous and miniature EPSC studies, the inter-EPSC interval, amplitude, area, decay time of 67% of the EPSC, and half-width duration were analyzed using Mini Analysis software (Synaptosoft, Decatur, GA), which detected events greater than 10 pA in amplitude. A Kolmogorov-Smirnov test (K-S test, Clampfit 10) was used to compare the preceding parameters in individual neurons, and a one-way ANOVA was used to compare group data. The amplitude, area, and half-width of evoked EPSCs were determined using Clampfit 10 and were further analyzed using Origin 8.0. Differences were considered significant at values of $P \leq 0.05$. All results are presented as mean ± SEM.

RESULTS

In this study, a total of 255 neurons were recorded in the SubCD, which is approximately 1 mm in diameter and located just anterior to the seventh nerve, caudal and medial to the PPN, as described previously (Figure 1A-B).[16-18] Recorded neurons were labeled with Lucifer yellow to confirm their locations in the SubCD (Figure 1C). In some experiments, stimulating electrodes were placed near afferent fibers to the SubCD. Figure

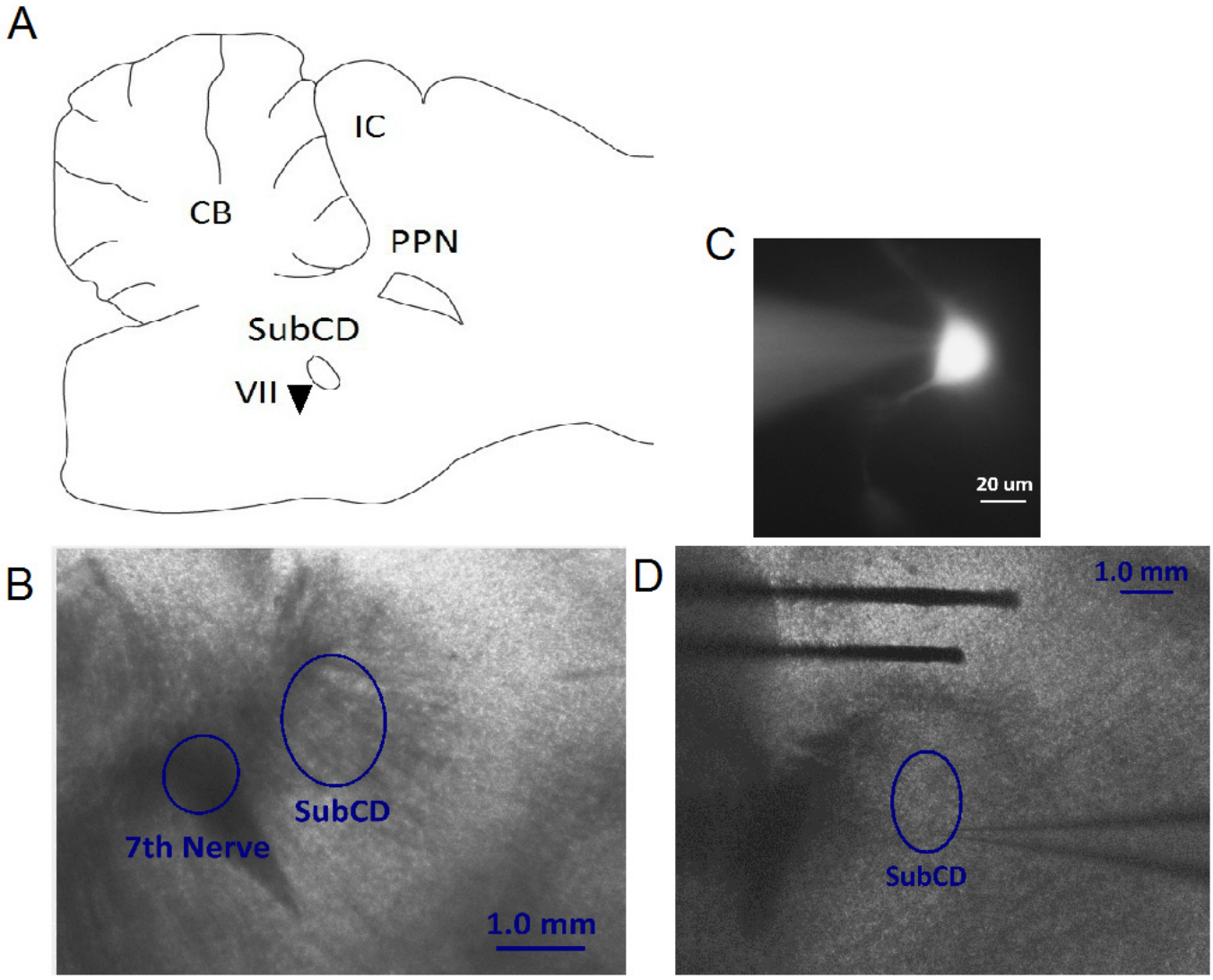

Figure 1—Location of recorded SubCD neurons. **(A)** Sagittal tissue sections containing the SubCD were used for recordings. **(B)** All SubCD neurons were located in a region anterior to the 7th nerve (calibration bar 1mm). **(C)** Recorded neurons were labeled with Lucifer yellow to confirm location in the SubCD (calibration bar 20 µm). **(D)** Photomicrograph of the SubCD and surrounding area showing the location of stimulating (lines at the top) and recording electrodes (outline left side). CB, cerebellum; IC, inferior colliculus; PPN, pedunculopontine nucleus; SubCD, dorsal subcoeruleus nucleus; VII, 7th nerve.

1D shows a photomicrograph of the location of the stimulating electrodes located dorsal to the SubCD, and the recording electrode located in the SubCD.

Afferents to the SubCD include the PPN and laterodorsal tegmental nucleus (LDT), and these afferents might include glutamatergic neurons.[4,8,9] We analyzed the effects of GLU receptor agonists on spontaneous EPSCs (Figure 2). A change in spontaneous EPSC amplitude or frequency following agonist exposure would indicate an activation of SubCD afferents and increased neurotransmitter release onto SubCD neurons. Prior to application of GLU receptor agonists, GBZ and STR were applied to block $GABA_A$ and glycine receptors, and ATR and MEC were applied to block ACh receptors. Therefore, we recorded the effects specifically of NMDA and KA on GLU release from presynaptic neurons onto SubCD neurons.

Application of KA and NMDA increased spontaneous EPSC frequency in 12/27 (44%) and 20/31 (65%) of the recorded neurons, respectively (K-S Test, $P < 0.05$). In the other neurons, no change in spontaneous EPSC frequency was observed. Perhaps the afferents of these neurons were cut during slice preparation, or the concentration of agonist was not sufficient to increase synaptic release. A representative recording revealed an increase in spontaneous EPSCs following KA (Figure 2A) or NMDA (Figure 2E), with an expanded recording (Figure 2B, 2F) before agonist exposure (top), during the peak effect of the agonist (middle), and following washout of the agonist (bottom). In this neuron, the cumulative probability distributions revealed a significant increase in both the frequency (K-S Test, $P < 0.001$) and amplitude (K-S Test, $P < 0.01$) of spontaneous EPSCs following KA or NMDA exposure (Figure 2C, 2G). In pooled data from all of the neurons, KA significantly increased the frequency (left) (1-way ANOVA, $f = 25.50$, $df = 34$, $P < 0.001$) and amplitude (right) (1-way ANOVA, $f = 8.64$, $df = 34$, $P < 0.001$) of spontaneous EPSCs (Figure 2D). NMDA also increased the frequency (left) (one-way ANOVA, $f = 38.64$, $df = 61$, $P < 0.001$) and amplitude (right) (1-way ANOVA, $f = 4.90$, $df = 61$, $P < 0.01$) (Figure 2H). Therefore, KA and NMDA appear to excite neu-

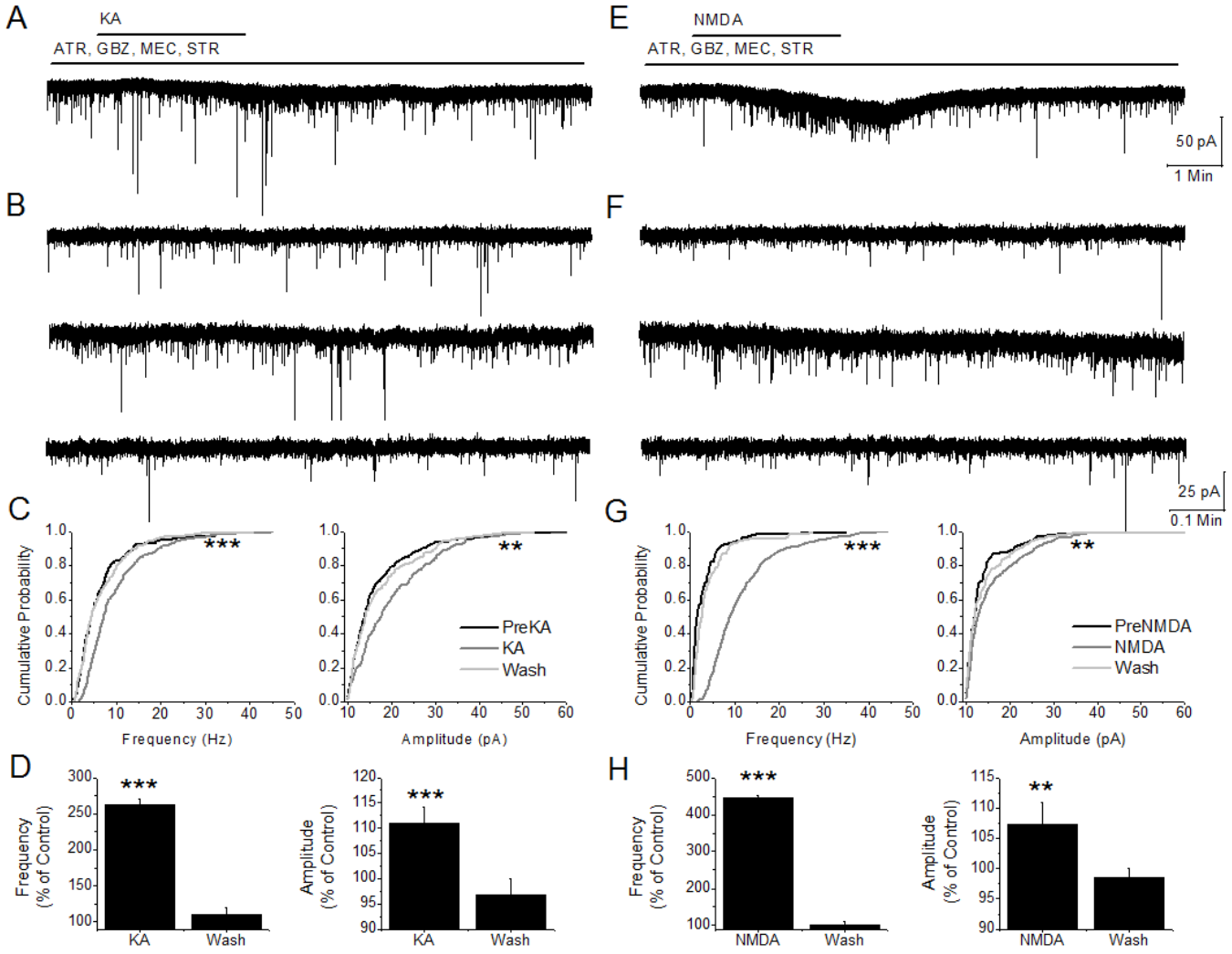

Figure 2—Effects of KA and NMDA receptor agonists on spontaneous EPSCs. **(A)** Representative recording showing changes in spontaneous EPSCs during KA exposure (top line), in comparison to ATR, GBZ, MEC, and STR (bottom line). **(B)** One-minute expanded recordings taken from A showing spontaneous EPSCs before KA exposure (top record), during the peak effect of KA (middle record), and following washout of KA (bottom record). **(C)** In this neuron, KA (gray lines) increased both the frequency (left) and amplitude (right) of spontaneous EPSCs compared to control (black lines) and washout (light gray lines). **(D)** Pooled data from all of the recorded neurons revealed a significant increase in spontaneous EPSC frequency (left graph) and amplitude (right graph) during KA exposure. **(E)** Representative recording showing changes in spontaneous EPSCs during NMDA exposure (top line), in comparison to ATR, GBZ, MEC, and STR (bottom line). **(F)** One-minute expanded recordings taken from E showing spontaneous EPSCs before NMDA exposure (top record), during the peak effect of NMDA (middle record), and following washout of NMDA (bottom). **(G)** In this neuron, NMDA (gray lines) increased both the frequency (left graph) and amplitude (right graph) of spontaneous EPSCs compared to control (black lines) and washout (light gray lines). **(H)** Pooled data from all of the recorded neurons revealed an increase in spontaneous EPSC frequency (left graph) and amplitude (right graph) following NMDA (*P < 0.05, **P < 0.01, ***P < 0.001).

rons that project to the SubCD, increasing the frequency of synaptic release onto SubCD neurons.

The previous study (spontaneous EPSCs) revealed an increase in spontaneous events following KA and NMDA, indicating these receptors are located on the cell bodies of afferent neurons. The effects of KA (n = 14) and NMDA (n = 15) on miniature EPSCs was also tested, which would indicate these agonists act on receptors located on glutamatergic terminals. These studies were performed in the presence of TTX, GBZ, STR, ATR, and MEC in order to record glutamatergic miniature EPSCs. Similar to the spontaneous EPSC findings, an increase in the frequency of miniature EPSCs was observed during KA (1-way ANOVA, $f = 5.79$, $df = 41$, $P < 0.01$), and NMDA exposure (1-way ANOVA, $f = 13.93$, $df = 44$, $P < 0.001$). No changes in miniature EPSC amplitude were observed following KA exposure (1-way ANOVA, $f = 1.54$, $df = 41$, $P > 0.05$), but an increase in miniature EPSC amplitude was observed during NMDA exposure (1-way ANOVA, $f = 7.83$, $df = 44$, $P < 0.001$). Therefore, KA and NMDA appear to excite receptors located on the axon terminals of glutamatergic afferents, increasing the frequency of miniature EPSCs.

To confirm that activation of SubCD afferents increases neurotransmitter release onto the SubCD, stimulating electrodes were placed near afferent fibers to the SubCD (Figure 1D). Stimulation of these fibers induced release of neurotransmitter onto the recorded SubCD neuron, and the response to GLU release was determined using receptor antagonists. Following application of GBZ and STR (Figure 3A), a large excitatory

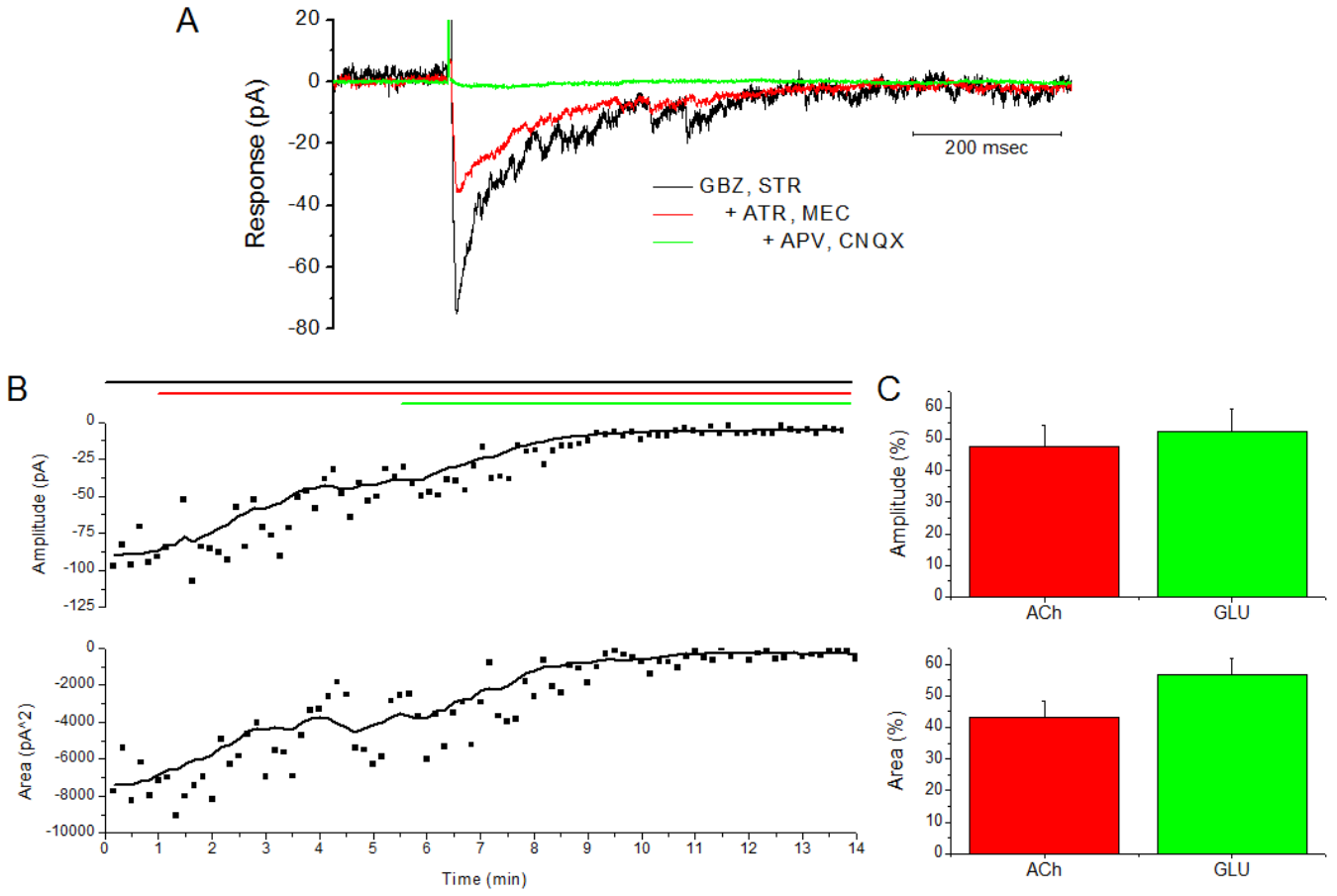

Figure 3—Role of KA and NMDA receptors in the evoked response. **(A)** Average of 10 evoked responses of a single SubCD neuron following stimulation during exposure to GBZ and STR (black record), added to block inhibitory neurotransmission, then ATR and MEC to block cholinergic transmission (red record), and finally APV and CNQX to block GLU transmission (green record). Note that cholinergic blockade blocked some of the response and GLU blockade blocked the remainder of the response. **(B)** Amplitude (top graph) and area (bottom graph) of the response during the entire recording. Colored bars represent the application time of each drug. The evoked EPSC amplitude and area increased slightly following GBZ and STR (black line at the top), decreased following ATR and MEC (red line at the top), and was blocked by APV and CNQX (green line at the top). **(C)** Pooled data from all of the recorded neurons showed the roughly equal contributions of ACh (red bars) and GLU (green bars) to the evoked EPSC amplitude (top graph) and area (bottom graph).

response was observed. Subsequent application of ATR and MEC blocked some of the evoked EPSC, and APV and CNQX blocked the remainder of the response. The amplitude (top) and area (bottom) of the response during the entire 14-min recording are shown in Figure 3B. In pooled data from all of the neurons (n = 8, Figure 3C), ACh mediated 47% ± 7% of the evoked EPSC amplitude (top) and 43% ± 5% of the evoked EPSC area (bottom). GLU mediated 53% ± 7% of the evoked EPSC amplitude (top) and 57% ± 5% of the evoked EPSC area (bottom). Therefore, stimulation of SubCD afferents evoked EPSCs in SubCD neurons, which were blocked by both ACh and GLU receptor antagonists.

To determine developmental changes in response to receptor agonists, KA (n = 44) and NMDA (n = 48) were applied to the bath and the effects on SubCD neurons were analyzed further (Figure 4). Application of KA (Figure 4A, top) or NMDA (Figure 4B, top) induced an inward current in all of the recorded neurons. A decrease in R_{in} was also observed following KA (Figure 4A bottom) and NMDA (Figure 4B bottom), indicating an increase in the number of channel openings during agonist exposure. The amplitude of the response was measured and averaged during 9-11 and 12-15 days (Figure 4C). A significant developmental decrease was observed in response to KA (2-sample *t*-test, $t = 3.22$, df = 42, $P < 0.01$), but no developmental changes were observed in response to NMDA (2-sample *t*-test, $t = 0.07$, df = 46, $P > 0.05$). No developmental changes in R_{in} were observed (Figure 4D) (2-sample *t*-test, $t = 1.62$, df = 47, $P > 0.05$). The response amplitude was normalized to the area of the neuron by calculating the current density (Figure 4E), which yields the response per unit area. When current density was compared across development, a significant developmental decrease in response to both KA (2-sample *t*-test, $t = 7.83$, df = 42, $P < 0.001$) and NMDA (2-sample *t*-test, $t = 2.15$, df = 46, $P < 0.05$) was observed. Therefore, there was a significant developmental decrease in the responses of SubCD neurons to both NMDA and KA.

This developmental decrease was confirmed by analyzing the direct effects of KA (n = 44) and NMDA (n = 48), using the voltage-dependent sodium channel blocker TTX, which blocks sodium channels and thus action potential generation (Figure 4F-H). The direct responses on the membrane of recorded SubCD neurons were consistent with the previous ex-

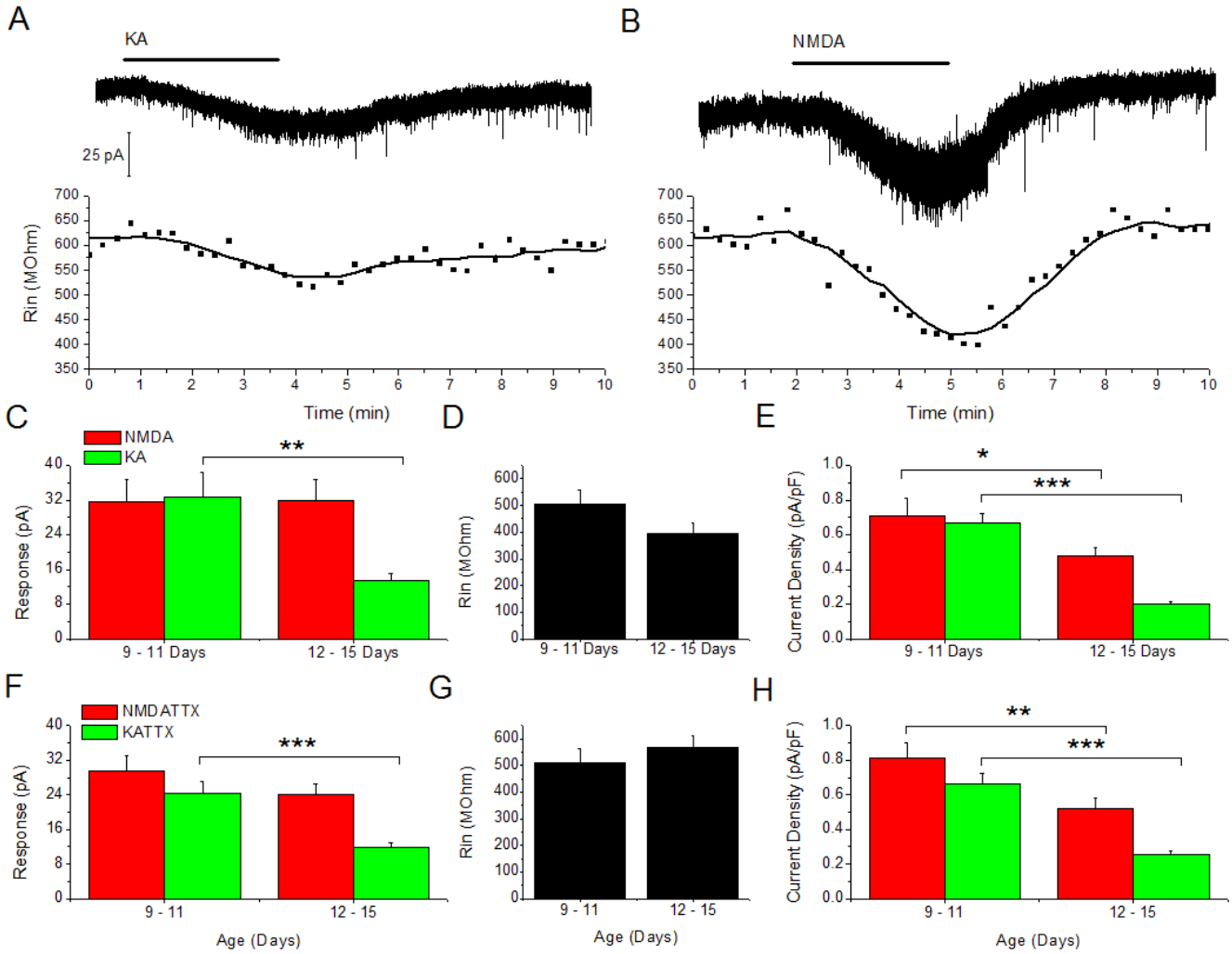

Figure 4—Response of SubCD neurons to GLU receptor agonists. **(A)** Recording during bath application of KA revealed an inward current in this neuron (top record) and a decrease in R_{in} (bottom graph). **(B)** An inward current (top record) and a decrease in R_{in} (bottom graph) was also observed following bath application of NMDA. **(C)** Average response amplitude following KA (green bars) or NMDA (red bars) at 9-11 and 12-15 days. Note the significant decrease in response to KA during development. **(D)** No significant developmental changes in R_{in} were observed during this time. **(E)** Response amplitude was normalized to capacitance by calculating the current density, which gives the response per unit area; this measure revealed that both the KA and NMDA responses decreased during development. **(F)** Average direct response amplitude during KA (green bars) or NMDA (red bars) exposure with TTX at 9-11 and 12-15 days. **(G)** No significant developmental changes in R_{in} were observed in these neurons during this developmental period. **(H)** Direct response amplitude was normalized to capacitance to calculate the current density; this measure revealed that both the KA and NMDA responses decreased during development (*P < 0.05, **P < 0.01, ***P < 0.001).

periment: a decrease in the response amplitude following KA (2-sample *t*-test, $t = 4.47$, df = 42, $P < 0.001$), no change in the response amplitude to NMDA (2-sample *t*-test, $t = 1.35$, df = 46, $P > 0.05$) (Figure 5F), no change in R_{in} (2-sample *t*-test, $t = 0.86$, df = 46, $P > 0.05$) (Figure 5G), and a decrease in current density in response to KA (2-sample *t*-test, $t = 6.69$, df = 42, $P < 0.001$) and NMDA (2-sample *t*-test, $t = 2.77$, df = 46, $P < 0.01$) (Figure 4H) was observed. Therefore, there appeared to be a developmental decrease in the response of SubCD neurons to both NMDA and KA.

Next, developmental changes in glutamatergic neurotransmission to the SubCD were analyzed using local stimulation to determine changes in synaptic GLU responses (n = 48, Figure 5). GBZ, STR, MEC, and ATR were applied at the beginning of each experiment to block inhibitory and cholinergic neurotransmission. The response of a neuron from a 10-day-old pup is shown in Figure 5A-B. Stimulation induced a large evoked EPSC in this neuron (Figure 5A), which was blocked by application of APV and CNQX. The evoked EPSC amplitude (top) and area (bottom) during the entire recording is shown below (Figure 5B). The contribution of GLU receptor subtypes to the evoked EPSC at 15 days was also analyzed (Figure 5C-D). Stimulation induced an evoked EPSC in a representative neuron (Figure 5C), which was blocked by application of the GLU receptor antagonists APV and CNQX. The evoked EPSC amplitude (top) and area (bottom) during the entire recording is shown below (Figure 5D). Similar to the effects observed at 10 days, both the NMDA and AMPA/KA receptor subtypes appear to be important for glutamatergic neurotransmission at this age.

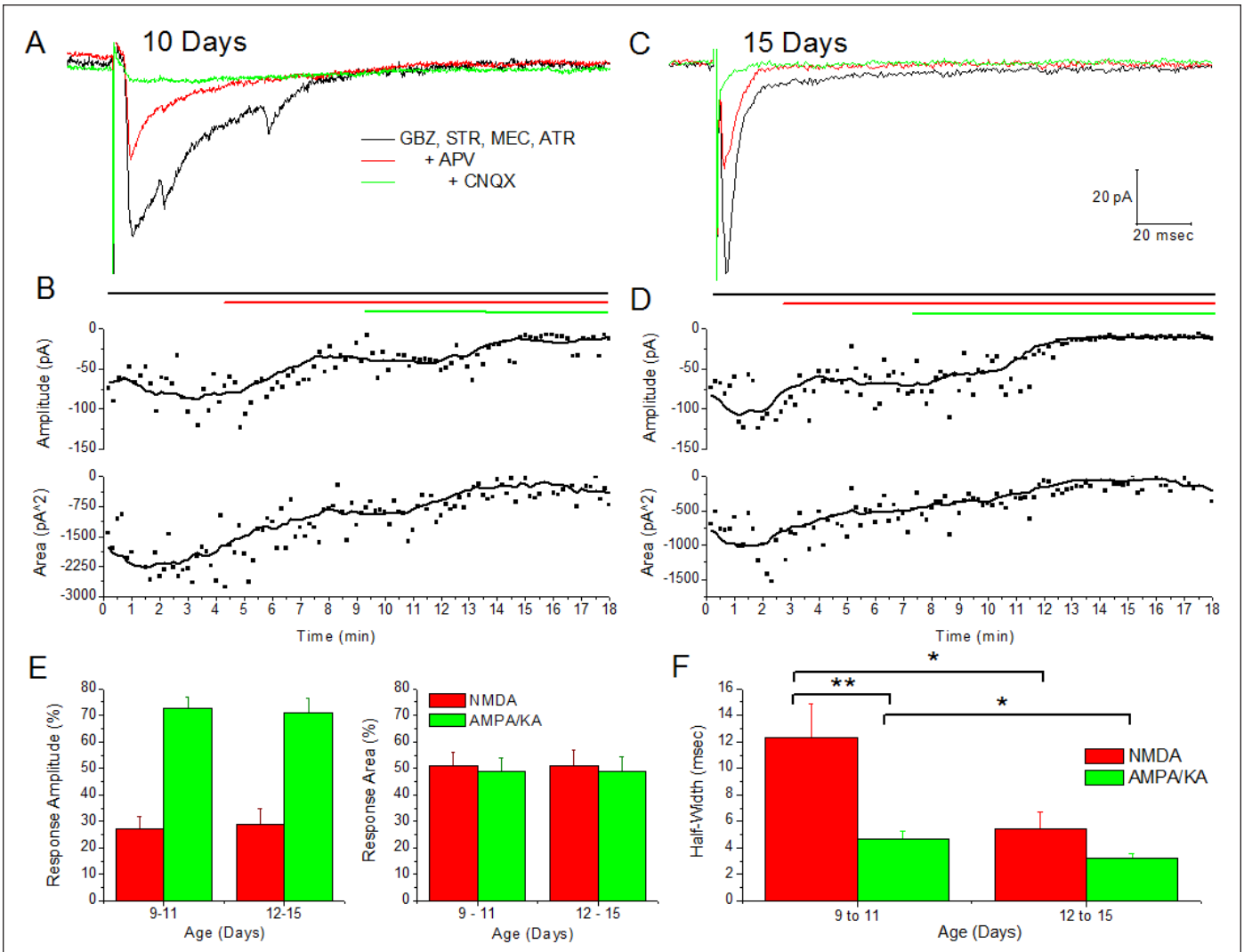

Figure 5—Developmental changes in the contribution of KA and NMDA to the evoked response. **(A)** Average of 10 evoked responses of a single neuron from a 10-day-old pup during GBZ, STR, ATR, and MEC (black record), during APV exposure (red record), which blocked part of the response, and during CNQX exposure (green record), which blocked the remainder of the response. **(B)** Evoked EPSC amplitude (top graph) and area (bottom graph) during the entire recording. The colored bars represent the application time of each drug. The evoked EPSC amplitude and area increased following GBZ, STR, ATR, and MEC (black line), decreased following APV (red line), and was blocked by CNQX (green line). **(C)** Average of 10 evoked response of a single neuron from a 15-day-old pup during GBZ, STR, ATR, and MEC (black record), during APV exposure (red record), and during CNQX exposure (green record). Note the reduced area of the response at 15 days compared to 10 days. **(D)** Evoked EPSC amplitude (top graph) and area (bottom graph) during the entire recording. The colored bars represent the application time of each drug. The evoked EPSC amplitude and area increased following GBZ, STR, ATR, and MEC (black), decreased following APV (red), and was blocked by CNQX (green). **(E)** Percentage of the evoked EPSC amplitude (left graph) and area (right graph) mediated by the NMDA (red bars) or KA (green bars) receptor during development (9-11 days vs. 12-15 days). **(F)** Half-width duration of the NMDA (red) and KA (green) components of the evoked EPSC during development (*P < 0.05, **P < 0.01, ***P < 0.001).

The percentage of the evoked EPSC amplitude (left) and area (right) mediated by NMDA or AMPA/KA receptors were compared during development (9-11 days [n = 24] vs. 12-15 days [n = 24], Figure 5E). At 9-11 days, the NMDA receptor mediated 27% ± 4% of the response amplitude, while the AMPA/KA receptor mediated 73% ± 4% of the evoked EPSC amplitude. No statistically significant changes were observed during 12-15 days, when the contribution of the NMDA receptor was 29% ± 6% and the AMPA/KA receptor 71% ± 6% of the response amplitude (2 sample *t*-test, $t = 0.24$, df = 46, $P > 0.05$). Similar results were observed when measuring the evoked EPSC area: at 9-11 days, the NMDA receptor mediated 50% ± 5% of the response area and AMPA/KA mediated 50% ± 5%; at 12-15 days, the NMDA receptor mediated 51% ± 6% of the response area and AMPA/KA mediated 49% ± 6% of the response area (2-sample *t*-test, $t = 0.28$, df = 46, $P > 0.05$). Therefore, the relative contribution of the NMDA and AMPA/KA receptor to the response of SubCD neurons to GLU does not appear to change during development.

While the contribution of the AMPA/KA and NMDA receptor to the evoked EPSC did not change during development, the size of the evoked EPSC appeared to decrease, but this could not be compared due to the variability between experiments (see Discussion). However, the half-width duration is not dependent on the stimulus intensity or number of presynaptic glutamatergic terminals and would not vary due to experimental condi-

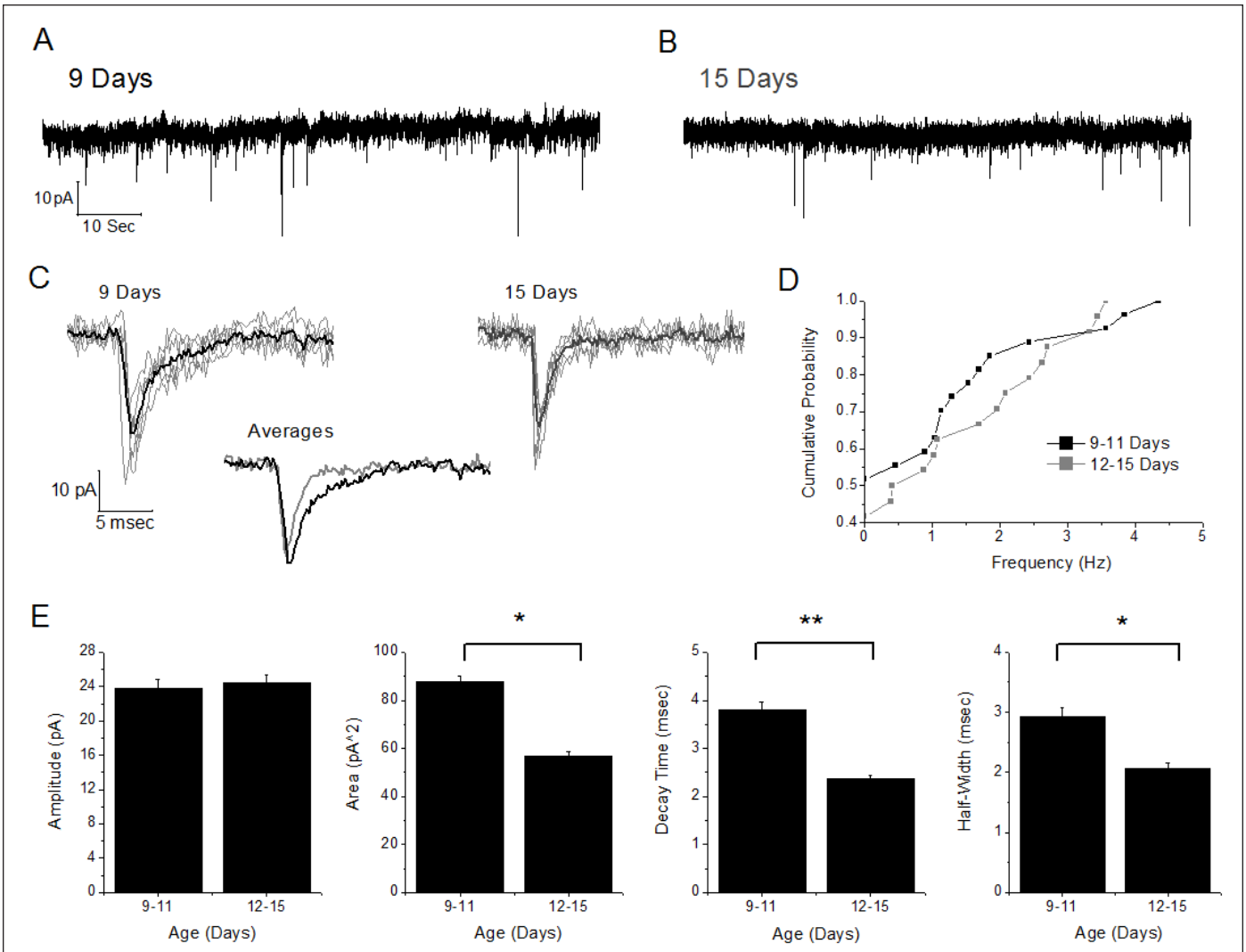

Figure 6—Developmental changes in miniature EPSCs. Glutamatergic mEPSCs were isolated using TTX, GBZ, STR, ATR, and MEC. **(A)** One-minute recording showing miniature EPSCs in a cell from a 9-day-old rat pup. **(B)** One minute recording show miniature EPSCs in a cell from a 15-day-old rat pup. **(C)** Average miniature EPSC at 9 days (left, thick black line) and 15 days (right, thick gray line), calculated by averaging 5 miniature EPSCs from A&B (gray). The two averages are superimposed below (9 days, black; 15 days, gray). **(D)** Cumulative probability distribution for the miniature EPSC frequency in all neurons at 9-11 days (black) and 12-15 days (gray). Note that ≈ 50% of the recorded neurons had a frequency of zero because they did not have miniature EPSCs. **(E)** Average amplitude, area, decay time, and half-width duration for the neurons with miniature EPSCs at 9-11 and 12-15 days (*P < 0.05, **P < 0.01, ***P < 0.001).

tions (Figure 5F). The half-width of the NMDA component of the evoked EPSC decreased from 12.30 ± 2.56 at 9-11 days to 5.43 ± 1.31 at 12-15 days (2-sample *t*-test, $t = 2.30$, df = 46, $P < 0.05$), while the AMPA/KA component decreased from 4.68 ± 0.57 to 3.25 ± 0.30 (2-sample *t*-test, $t = 2.22$, df = 46, $P < 0.05$). Therefore, the half-width duration of both the NMDA and AMPA/KA component of the evoked EPSC decreases during development.

To confirm developmental changes in synaptic GLU responses, changes in miniature EPSCs, which represent spontaneous release of neurotransmitter, were recorded in the presence of TTX, GBZ, STR, ATR, and MEC in order to isolate glutamatergic miniature EPSCs. Considering these experiments were performed in Mg^{2+} aCSF, the miniatures are likely mediated by NMDA, AMPA, and KA receptors. Glutamatergic miniature EPSCs were observed in 14/27 (52%) of the recorded neurons at 9-11 days and 14/24 (58%) at 12-15 days (Figure 6 A-B), and the miniature EPSCs observed at 9-11 days appeared to have slower decay times than those recorded at 12-15 days (Figure 6C). The frequency of miniature EPSCs was compared for all recorded neurons at 9-11 and 12-15 days, including neurons with no miniature EPSCs, since there could be a developmental change in the number of neurons exhibiting glutamatergic miniature EPSCs (Figure 6D), and no developmental changes were observed (K-S Test, $P > 0.05$). In the neurons with miniature EPSCs, there were no developmental changes in the amplitude (2-sample *t*-test, $t = 0.29$, df = 26, $P > 0.05$), but there was a significant development decrease in the area (2-sample *t*-test, $t = 2.81$, df = 26, $P < 0.05$), decay time (2-sample *t*-test, $t = 3.97$, df = 26, $P < 0.01$), and half-width duration (2-sample *t*-test, $t = 2.91$, df = 26, $P < 0.05$). Therefore, there appears to be developmental changes in the kinetic properties of synaptic GLU responses.

DISCUSSION

This study describes the role of glutamatergic neurotransmission in the excitation of SubCD neurons in vitro. Bath ap-

plication of NMDA or KA increased GLU-elicited spontaneous and miniature EPSCs in SubCD neurons, indicating that GLU receptor agonists excite neurons that project to the SubCD and increase GLU release from these neurons. Glutamatergic afferents were conformed using electrical stimulation of SubCD afferent axons, which induced an evoked EPSC blocked by ACh and GLU receptor antagonists. A development decrease in the response of SubCD neurons was observed following bath application of KA or NMDA, but no developmental changes were observed in the relative contribution of AMPA/KA or NMDA receptors to the evoked EPSC. However, a development decrease in the half-width duration of the evoked EPSCs and area, decay time, and half-width duration of miniature EPSCs were observed. Glutamatergic input to the SubCD appears to activate these REM-on neurons, which could play a role in REM sleep generation in vivo.

Pharmacological (Figure 2) or electrical (Figs. 3 and 5) stimulation of SubCD afferents would likely induce the release of a number of neurotransmitters into the SubCD. However, recordings of spontaneous and miniature EPSCs were performed in the presence of GBZ, STR, ATR, and MEC to block $GABA_A$, glycine, and ACh receptors, respectively. Therefore, it is likely we measured only changes in GLU-elicited spontaneous and miniature EPSCs. Likewise, electrical stimulation studies were performed in the presence of GBZ and STR, and the evoked EPSC was blocked by ACh and GLU receptor antagonists. Cholinergic neurotransmission in the SubCD has previously been described in vitro.[15,16] Spontaneous, miniature, and evoked EPSCs were likely mediated by NMDA, AMPA, and KA receptors, since Mg^{2+}-free aCSF was used for all recordings.

To determine developmental changes, KA or NMDA were applied to the bath (Figure 4). In some experiments, TTX was applied to block voltage-dependent sodium channels and observe the direct effects of agonists on the recorded neuron. In these experiments, no significant developmental changes were observed in the direct response to NMDA, but a significant developmental decrease was observed when comparing the current density, a measure of the current per unit area of the neuron. Previous experiments revealed the presence of both large and small glutamatergic neurons in the SubCD,[10] but changes in cell size during development were not measured. Perhaps we recorded from a mixture of small and large neurons at each point in development, which would lead to a range of direct response amplitudes with a similar average. A significant developmental decrease was also observed in response to KA, which could explain the findings observed in Figure 5; the ratio of the receptor subtypes mediating the evoked EPSC remained constant during development because both were decreasing in receptor sensitivity, receptor number, or some other mechanism.

Local electrical stimulation (Figure 5) likely activated nearby SubCD axons and induced release of neurotransmitter onto the recorded neuron. Like previous studies (Figs. 2 and 3), this experiment was performed in the presence of GBZ, STR, ATR, and MEC to localize the GLU-elicited evoked EPSC. Indeed, the evoked EPSC was blocked by APV and CNQX. Considering bath application of agonist activates all receptors on the neuron (synaptic and extrasynaptic), evoked and miniature EPSCs is a preferred method for measuring developmental changes in synaptic responses. Evoked EPSC studies revealed no significant developmental changes in the ratio of AMPA/KA and NMDA receptors mediating the evoked EPSC. However, because of the variability between evoked EPSC experiments (distance of the electrode, stimulation threshold, and location of nearby neurons), we did not measure changes in the amplitude or area of the evoked EPSC during development, only the ratio of AMPA/KA and NMDA receptor contribution. There was a significant decrease in the half-width duration, and the amplitude and area of the evoked EPSC did appear to decrease during development, which may be expected considering the developmental decrease in response to both KA and NMDA observed in other experiments (Figure 4).

A significant developmental decrease in the area, decay time, and half-width duration also was observed in miniature EPSC studies (Figure 6). However, longer half-width durations were observed during evoked EPSCs studies. Miniature EPSCs result from spontaneous release from one axon terminal. On the other hand, electrical stimulation likely activated a number of axons, leading to asynchronous release from multiple axon terminals, with the timing of release dependent on the conduction velocity of each axon. Furthermore, proximity of the synapse to the cell body affects EPSC properties, with synapses closer to the cell body displaying larger amplitudes and slower decay times and more distal synapses displaying smaller amplitudes and larger decay times.

Similar developmental changes have been observed between postnatal days 5 and 14 in the auditory brainstem, where NMDA and AMPA receptor-mediated EPSCs acquired faster decay kinetics, with no change in the mean amplitude of AMPA receptor-mediated EPSCs.[19] These developmental changes in NMDA receptors may be explained by a modification of the subunit composition during development. Indeed, the NR2B subunit of the NMDA receptor predominates early in development and is later replaced by the NR2A subunit.[20] In the neocortex, neurons expressing the NR2A-containing NMDA receptors had faster NMDA receptor-mediated EPSCs,[21] and transfection of mammalian HEK cells also revealed faster kinetics in NR2A-containing NMDA receptors.[22] Therefore, the developmental decrease in direct agonist effect, evoked EPSC, and miniature EPSC studies may be due to changes in the kinetics of GLU receptors in the SubCD. Alternative explanations to the developmental decrease in kinetic properties of EPSCs could be an increase in transporter-mediated glutamate uptake or receptor desensitization.

Physiological Significance

Many studies have revealed the importance of the SubCD in the generation of REM sleep, muscle atonia, and PGO waves. Activation of the SubCD induced REM sleep with muscle atonia and PGO waves,[1-5] while inactivation of this area produced REM sleep without muscle atonia[6] or decreased REM sleep.[23] The SubCD sends descending glutamatergic projections to inhibitory glycinergic medullary neurons, which inhibit motoneurons during REM sleep.[24,25] In humans, pontine strokes that include the SubCD result in REM sleep behavior disorder (RBD),[26] which is characterized by the loss of muscle atonia during REM sleep. It has been hypothesized that RBD is a result of degeneration of glutamatergic SubCD neurons, or their targets in the medulla.[24]

One potential source of glutamatergic input to the SubCD is the PPN, which contains glutamatergic neurons that are excited by GLU receptor agonists.[7,27] Microinjections of GLU into the PPN of the freely moving rat increased both REM sleep and waking,[28] NMDA specifically increased waking,[29] and KA specifically increased REM sleep,[30,31] which is protein kinase A-dependent.[32] On the other hand, injections of antagonists for the AMPA receptor or metabotropic receptors had no effect on sleep/wake states in the rat.[30,31] In the SubCD, microinjections of KA induced a REM sleep-like state with muscle atonia,[4] but GLU and NMDA have yet to be tested. Perhaps GLU and NMDA would also increase REM sleep, but our results predict that there would be a developmental decrease in the amount of REM sleep induced by these agonists.

Previously, we characterized the roles of the KA and NMDA receptors in excitation of PPN neurons in vitro.[27] In pharmacological and electrical stimulation studies, a developmental increase in the response mediated through the KA receptor and developmental decrease in the response mediated through the NMDA receptor was observed.[27] In contrast, we observed a developmental decreased in both the NMDA and KA receptors in the SubCD. There is a developmental decrease in REM sleep that occurs in humans from birth until puberty,[14] and in rats from 10-30 days of age.[13] A developmental decrease in the excitatory responsiveness of REM-on neurons in the SubCD neurons may be implicated in this decrease in REM sleep. Furthermore, we were only able to record from neurons during a limited age range (9-15 days), due to difficultly visualizing the neurons after 15 days. Perhaps these developmental changes would continue in older animals before reaching a steady state at 30 days, when developmental changes maximally decline in the rat. Briefly, it appears that glutamatergic input to PPN may be more related to differential changes in state between waking and REM sleep, whereas the same input to SubCD may be more related to the developmental decrease in REM sleep.

ABBREVIATIONS

ACh, acetylcholine
aCSF, artificial cerebral spinal fluid
AMPA, 2-amino-3-(5-methyl-3-oxo-1,2-oxazol-4-yl) propanoic acid
APV, 2-amino-5-phosphonovaleric acid
ATR, atropine
BIC, bicuculline
CAR, carbachol
CNQX, 6-cyano-7-nitroquinoxaline-2,3-dione
EEG, electroencephalogram
EPSC, excitatory post-synaptic current
GABA, gamma aminobutyric acid
GBZ, gabazine
GLU, glutamate
KA, kainic acid
K-S test, Kolmogorov-Smirnov test
LDT, laterodorsal tegmental nucleus
MEC, mecamylamine
NMDA, N-methyl-D-aspartic acid
PGO, waves ponto-geniculo-occipital waves
PPN, pedunculopontine nucleus
RBD, REM sleep behavior disorder
REM, rapid eye movement sleep
R_{in}, input resistance
SE, standard error
SubCD, dorsal subcoeruleus nucleus
TTX, tetrodotoxin

ACKNOWLEDGMENTS

This work was supported by NIH awards R01 NS020246, and by core facilities of the Center for Translational Neuroscience supported by P20 RR020146.

DISCLSOURE STATEMENT

This was not an industry supported study. The authors have indicated no financial conflicts of interest.

REFERENCES

1. Baghdoyan HA, Rodrigo-Angulo ML, McCarley RW, Hobson JA. A neuroanatomical gradient in the pontine tegmentum for the cholinoceptive induction of desynchronized sleep signs. Brain Res 1987;414:245-61.
2. Vanni-Mercier G, Sakai K, Lin JS, Jouvet M. Mapping of cholinoceptive brainstem structures responsible for the generation of paradoxical sleep in the cat. Arch Ital Biol 1989;127:133-64.
3. Datta S, Siwek DF, Patterson EH, Cipolloni PB. Localization of pontine PGO wave generation sites and their anatomical projections in the rat. Synapse 1998;30:409-23.
4. Boissard R, Gervasoni D, Schmidt MH, Barbagli B, Fort P, Luppi PH. The rat ponto-medullary network responsible for paradoxical sleep onset and maintenance: a combined microinjection and functional neuroanatomical study. Eur J Neurosci 2002;16:1959-73.
5. Pollock MS, Mistlberger RE. Rapid eye movement sleep induction by microinjection of the GABA-A antagonist bicuculline into the dorsal subcoeruleus area of the rat. Brain Res 2003;962:68-77.
6. Sanford LD, Yang L, Tang X, Ross RJ, Morrison AR. Tetrodotoxin inactivation of pontine regions: influence on sleep-wake states. Brain Res 2005;1044:42-50.
7. Wang HL, Morales M. Pedunculopontine and laterodorsal tegmental nuclei contain distinct populations of cholinergic, glutamatergic and GABAergic neurons in the rat. Eur J Neurosci 2009;29:340-58.
8. Datta S, Patterson EH, Siwek DF. Brainstem afferents of the cholinoceptive pontine wave generation sites in the rat. Sleep Res Online 1999;2:79-82.
9. Boissard R, Fort P, Gervasoni D, Barbagli B, Luppi PH. Localization of the GABAergic and non-GABAergic neurons projecting to the sublaterodorsal nucleus and potentially gating paradoxical sleep onset. Eur J Neurosci 2003;18:1627-39.
10. Clement O, Sapin E, Berod A, Fort P, Luppi PH. Evidence that neurons of the sublaterodorsal tegmental nucleus triggering paradoxical (REM) sleep are glutamatergic. Sleep 2011;34:419-23.
11. Datta S, Siwek DF, Stack EC. Identification of cholinergic and non-cholinergic neurons in the pons expressing phosphorylated cyclic adenosine monophosphate response element-binding protein as a function of rapid eye movement sleep. Neuroscience 2009;163:397-414.
12. Verret L, Leger L, Fort P, Luppi PH. Cholinergic and noncholinergic brainstem neurons expressing Fos after paradoxical (REM) sleep deprivation and recovery. Eur J Neurosci 2005;21:2488-504.
13. Jouvet-Mounier D, Astic L. [Study of the course of sleep in the young rat during the 1st postnatal month]. C R Seances Soc Biol Fil 1968;162:119-23.
14. Roffwarg HP, Muzio JN, Dement WC. Ontogenetic development of the human sleep-dream cycle. Science 1966;152:604-19.
15. Brown RE, Winston S, Basheer R, Thakkar MM, McCarley RW. Electrophysiological characterization of neurons in the dorsolateral pontine rapid-eye-movement sleep induction zone of the rat: Intrinsic membrane properties and responses to carbachol and orexins. Neuroscience 2006;143:739-55.
16. Heister DS, Hayar A, Garcia-Rill E. Cholinergic modulation of GABAergic and glutamatergic transmission in the dorsal subcoeruleus: mechanisms for REM sleep control. Sleep 2009;32:1135-47.

17. Heister DS, Hayar A, Charlesworth A, Yates C, Zhou YH, Garcia-Rill E. Evidence for electrical coupling in the subcoeruleus (subc) nucleus. J Neurophysiol 2007;97:3142-7.
18. Simon C, Kezunovic N, Williams DK, Urbano FJ, Garcia-Rill E. Cholinergic and glutamatergic agonists induce gamma frequency activity in dorsal subcoeruleus nucleus neurons. Am J Physiol Cell Physiol 2011;301:C327-35.
19. Taschenberger H, von Gersdorff H. Fine-tuning an auditory synapse for speed and fidelity: developmental changes in presynaptic waveform, EPSC kinetics, and synaptic plasticity. J Neurosci 2000;20:9162-73.
20. Cull-Candy S, Brickley S, Farrant M. NMDA receptor subunits: diversity, development and disease. Curr Opin Neurobiol 2001;11:327-35.
21. Flint AC, Maisch US, Weishaupt JH, Kriegstein AR, Monyer H. NR2A subunit expression shortens NMDA receptor synaptic currents in developing neocortex. J Neurosci 1997;17:2469-76.
22. Vicini S, Wang JF, Li JH, et al. Functional and pharmacological differences between recombinant N-methyl-D-aspartate receptors. J Neurophysiol 1998;79:555-66.
23. Karlsson KA, Gall AJ, Mohns EJ, Seelke AM, Blumberg MS. The neural substrates of infant sleep in rats. PLoS Biol 2005;3:e143.
24. Luppi PH, Clement O, Sapin E, et al. The neuronal network responsible for paradoxical sleep and its dysfunctions causing narcolepsy and rapid eye movement (REM) behavior disorder. Sleep Med Rev 2011;15:153-63.
25. Morales FR, Sampogna S, Rampon C, Luppi PH, Chase MH. Brainstem glycinergic neurons and their activation during active (rapid eye movement) sleep in the cat. Neuroscience 2006;142:37-47.
26. Xi Z, Luning W. REM sleep behavior disorder in a patient with pontine stroke. Sleep Med 2009;10:143-6.
27. Simon C, Hayar A, Garcia-Rill E. Responses of developing pedunculopontine neurons to glutamate receptor agonists. J Neurophysiol 2011;105:1918-31.
28. Datta S, Spoley EE, Patterson EH. Microinjection of glutamate into the pedunculopontine tegmentum induces REM sleep and wakefulness in the rat. Am J Physiol Regul Integr Comp Physiol 2001;280:R752-9.
29. Datta S, Patterson EH, Spoley EE. Excitation of the pedunculopontine tegmental NMDA receptors induces wakefulness and cortical activation in the rat. J Neurosci Res 2001;66:109-16.
30. Datta S. Evidence that REM sleep is controlled by the activation of brain stem pedunculopontine tegmental kainate receptor. J Neurophysiol 2002;87:1790-8.
31. Datta S, Spoley EE, Mavanji VK, Patterson EH. A novel role of pedunculopontine tegmental kainate receptors: a mechanism of rapid eye movement sleep generation in the rat. Neuroscience 2002;114:157-64.
32. Datta S, Desarnaud F. Protein kinase A in the pedunculopontine tegmental nucleus of rat contributes to regulation of rapid eye movement sleep. J Neurosci 2010;30:12263-73.